On the Pyramidal Faces of Ice Crystals*

by

Teisaku KOBAYASHI

Meteorological Section, Institute of Low Temperature Science

and

Keiji HIGUCHI

Department of Geophysics, Faculty of Science, Hokkaido University

(Manuscript Received Sept. 1957)

I. Introduction

Since SCORESBY[1] discovered an ice crystal of pyramid type in the Arctic, researches concerning such crystals have been carried out by a number of workers. HUMPHREYS[2] pointed out that the formation of halos of unusual radii was due to the refraction by the pyramidal faces of ice crystals constituting the upper clouds. NAKAYA[3] investigated the snow crystals by the method of photomicroscopy, and proposed the general classification of their types. In his classification, pyramid and bullet crystals were considered to have the pyramidal faces, though their facial angles were left undetermined. WEICKMANN[4] made a statistical measurement of the angles between pyramidal faces and principal axis as observed in the photographs of the ice crystals which constituted the cirrostratus cloud. WEICKMANN[4], SHAW and MASON[5] observed columnar crystals with pyramidal faces during the experiment of producing ice crystals on a metal plate. ITOO[6], in Manchuria, also found irregular forms of ice crystals in the air, of which he took the photographs and which he considered to have pyramidal and high index faces.

Now we have performed an analysis of various types of ice crystals having pyramidal faces, which made their appearance in the hoar, as shown in Photo. 1, artificially produced in a diffusion cloud chamber. The hoar was formed on a slide glass which was set at the side wall of the chamber originally used by one of the authors[7] for the investigation of snow-crystal habit and growth. The procedure of analysis consisted in classifying the crystal forms according to the variation in type of etch pits[8].

II. Experimental procedures

The apparatus and the conditions under which the crystals were produced are

* Contribution No. 388 from the Institute of Low Temperature Science.

as follows.

The main part of our diffusion cloud chamber is constructed of double walls of transparent Acrylite* for the facility of observation. The bottom made of thick copper walls, upon which the Acrylite walls are placed, is immersed in a cold brine-bath. The temperature of the brine-bath (T_b) is maintained at any desired temperature down to −40°C, by the aid of a refrigerating machine charged with Freon 22. Since the inner walls of the copper box are always covered with the frozen droplets sprayed by an atomizer, the air within the box is maintained approximately at ice saturation. The top of the chamber is covered with a number of sheets of wetted gauze serving as the water-vapour source, the temperature of which (T_w) can be regulated by electric heating up to 40°C. The condition of the air inside the chamber remains very stable without any convection or turbulence.

When the chamber, once operated, was left undisturbed half a day long, practically all the supercooled cloud droplets were rained out, and considerably high supersaturation in only vapour phase was realized. By adjusting T_b and T_w, any desired temperature (and corresponding vapour-density) profile could be observed in the chamber.

The slide glass, which was coated with Dri-film and baked at 160°C in electric

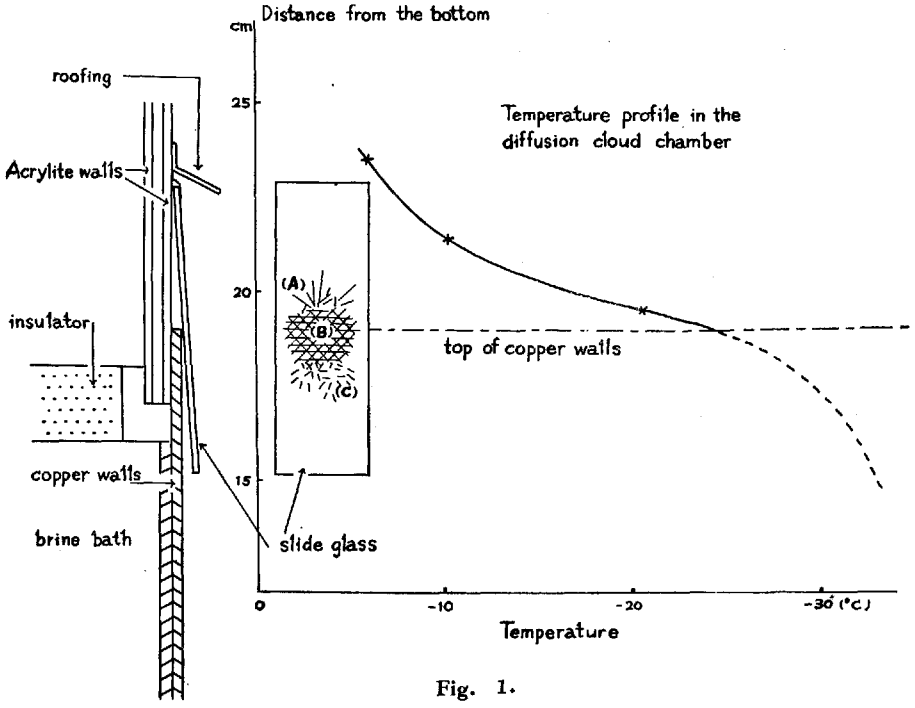

Fig. 1.

* Acrylic-acid resin.

oven for one hour, was placed with its coated surface inwards, against the Acrylite wall in such a position that it extended beyond the junction of the wall with the copper box. Just above the slide glass, a shelter of Valflon* plate was put on the wall so as to prevent any condensed water drop from running down the slide. Fig. 1 shows schematically the location of the slide on the wall and the mode of hoar-frost development on the slide.

Temperature profile of the air, which was determined by the use of three fine thermometers horizontally mounted 6 cm distant from the wall, is also shown in Fig. 1. The temperature gradient and consequently the supersaturation, was found to be the largest at the level near the top of the copper wall. But it must be noticed that the temperature distribution over the slide might considerably differ from that of the air layer, inasmuch as the central portion of the slide was in line contact with the edge of the copper wall, whose temperature (ca. −30°C) must have been lower than that of the air at the same level.

When the slide glass was left as it was, for twenty hours, the hoar frost appeared most densely within a relatively narrow region where the slide glass touched the edge of the copper wall, and rapidly decreased in density on both sides.

Since the air temperature of the room, where the diffusion cloud chamber was set up, was more or less higher than 0°C, measures had to be taken to prevent the hoar crystals from melting and being deformed during microscopic observation and photomicrography. A Petri dish of liquid paraffin saturated with distilled water was previously chilled down to −5°C in a low-temperature room, and was brought near to the diffusion chamber, before the upper lid of the chamber was removed. Upon removal of the lid the dish was put in the chamber and the slide was quickly immersed in the paraffin. The dish was brought back to the low-temperature room, in which the hoar crystals on the slide, as they were in the paraffin, were carefully examined by a microscope under illumination through an infrared-absorbing filter.

III. Observations

Since 1955, a series of snow-making experiments has been carried out by making use of the diffusion cloud chamber. We have thoroughly examined the snow-crystal forms produced under aerosol-free condition, controlling the ambient air temperature and supersaturation of water vapour. Recently it was found that the snow-crystal habit in aerosol-free air can approximately be represented by the so-called NAKAYA T_a—s diagram, and that the sheath- or needle-type growth, described in a previous paper[9], was due to the influence of the vapour trace of Dri-film which was used for the hydrophobic coating of the inner walls of the chamber. The effect of Dri-film vapour was confirmed owing to the kind suggestion offered by NAKAYA[10] and Hanazima who had found that the vapour trace of silicone oil remarkably affected

* Tetrafluoroethylene resin.

the snow-crystal habit. Subsequently various kinds of silicone oil, silicone grease or the like were put to the test by one of the authors with a view to clarifying the influence of these vapours upon the snow-crystal growth. As the result, it was redemonstrated that a trace of foreign vapours, especially of silicone oil or acetone, produces the most remarkable effects.

Methyl silicone oil* of low viscosity proved to be most favourable for the sheath-type growth (Photos. 2 and 3) and methyl-phenyl silicone oil** yielded a curious form of crystal (Photos. 6 and 7). Silicone oil of higher viscosity and silicone grease gave off no vapour, but a peculiar type of ice crystals was observed to grow on a fine thread or on a cotton ball wetted with them (Photo. 5.) The influence of Dri-film*** vapour was also found to be very remarkable. When a glass rod coated with a drop of Dri-film was inserted into the chamber, only sheath- or blade-type crystals were formed in the whole range of the temperature down to −35°C (Photo. 4).

The surface treated with Dri-film was then put to a similar test. A slide glass coated with Dri-film and baked at 160°C for an hour had no influence on the crystal habit, contrary to the case of non-baked surface. Ordinary sector or dendritic crystals grew under proper conditions on the rabbit hair, which was suspended near the central part of the chamber. On the slide glass itself there appeared, as will be fully described below, hoar crystals quite different in form from those on the rabbit hair.

Now that the hoar frost on the slide glass treated with hydrophobic substances such as Dri-film forms in itself an interesting object to be studied, the form of the hoar crystals was carefully examined following the procedure described in the preceding section.

The ice crystals observed on the slide glass are without doubt the hoar frost but not the precipitating ice crystals. When the slide was put in the chamber, it is true, numerous cloud droplets were formed because of unavoidable intrusion of moist room air into the chamber, but they were almost rained out in a few hours. The probability of the falling particles being captured by the surface of the slide, might well be assumed to be negligible, because the slide was set vertically under

---

* Linear methylpolysiloxanes, $CH_3-Si(CH_3)_2-O-[Si(CH_3)_2-O]_n-Si(CH_3)_2-CH_3$.

DC 200 (Dow Corning Co., 3, 10 c.s.), TS 951 (Tokyo Shibaura Electric Co., 0.65, 10, 100, 1000, 10000 c.s.) and KF 96 (Shin-etsu Kagaku Co., 5 c.s.) were used. Those which have viscosities less than 5 c.s. remarkably affected the snow crystal habit.

** Supplied by Tokyo Shibaura Electric Co., 6 c.s., $CH_3-Si(CH_3)_2-O-Si(C_6H_5)_2-O-Si(CH_3)_2-CH_3$.

*** A mixture of methyldichlorosilanes, produced and marketed by General Electric Co.

the roofing. The surface of the slide treated with Dri-film may be considered to have a molecular arrangement as illustrated in Fig. 2, whose remarkable water-repellent action is to be attributed to the oriented layer of methyl groups.

The hydrophobic (kryophobic[11]) surfaces may probably favour the formation of isolated germs, of which the major or *c*-axis is oriented parallel or inclined away from the treated surface at an acute angle, contrary to the case of kryophilic surface where the germs are oriented perpendicular to the surface. The crystal formed on the kryophobic surface, seems to develop only through sublimation (solidification from the vapour phase) growing upward from the small area where the crystal germ was initially produced.

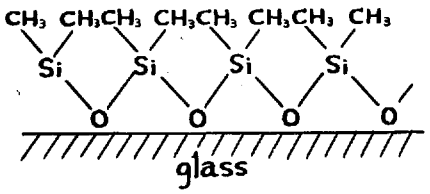

Fig. 2.

As regards the forms of crystals as well as the mode of development of the hoar frost, there was a considerable difference between the central narrow region (*B*) and the two neighbouring regions (*A* and *C*) of the slide glass (cf. Fig. 1).

In the region (*A*) of the slide surface, where the temperature was considerably higher than other regions, there appeared a kind of needle crystal, relatively few in number but large in size, growing parallel to the surface. Photo. 8 shows the needle crystals formed in this region.

The central region (*B*), where the temperature was probably the lowest, was most densely covered with isolated small crystals, consisting of hexagonal columns, columns with hexagonal pyramid, and their various modifications bounded by pyramidal faces. Photos. 14~17 are low-magnification photomicrographs of this region. In Photos. 20~29, which are the higher magnification of the same region, are revealed various types of hoar crystal apparently with pyramidal faces or high index faces. Several examples of these crystals will be fully illustrated in the following section.

At the lower marginal portion of the region (*B*), that is, in the region (*C*), many clumps of "flat" columnar or needle-like crystals are observed to grow from common germs in several directions. Photos. 18, 19, 30 and 31 illustrate such clumps of crystals.

Photomicrographs 14~31 were taken of the hoar crystals developed on one and the same slide. The slides treated with Dri-film were repeatedly put to the test, but the general mode of frost formation came out always the same, although sometimes the crystals formed in region (*B*) were so dense that their forms could not

be distinguished from one another; in some cases there were observed in region (*C*) relatively large crystals such as shown in Photos. 9~13. It was on one of four test slides that such fine crystals as shown in Photos. 14~31 manifested themselves. Although the question remains for solution how such crystals can be formed at all, it may well be worth while to give a detailed description of the crystal development on the kryophobic surfaces.

IV. Forms of ice crystals having pyramidal faces

As shown in the foregoing photographs, there are various forms of ice crystals. For the present, we shall deal mainly with the variation in shape of the crystals having pyramidal faces, as one of the authors[8] has classified the shapes of etch pits in relation to pyramidal faces. A hexagonal column and its variations obtained by the addition of pyramidal faces to it, are shown by the sketches in Fig. 3 (at the end of this paper), in which the pyramidal faces are indicated by hatching. Photos. 32~48, enlargements of foregoing photographs, afford an illustration of such crystals.

In Fig. 3 (1) is shown a hexagonal column, as a standard shape. Photo. 32 is a side view of the column, which is the same as the types observed by WEICKMANN[4] and ITOO[12]. It is noteworthy that these hexagonal columns are similar to the columnar crystals of snow[13], except that there are no hollows on the bases, and that they have the same shape as the minute solid needle of artificial snow described by NAKAYA[14]. Photo. 33 shows the end view of the short column, which may be a thick plate. Fig. 3 (2) is a hexagonal column with one pyramidal face. The side views of such a crystal are illustrated in Photo. 34 and Photo. 35, the latter being the side view from the direction parallel to *a*-axis. Fig. 3 (3) is a hexagonal column with two pyramidal faces, $(1\bar{1}01)$ and $(01\bar{1}1)$, and Photo. 36 is an actual example. Fig. 3 (4) is a hexagonal column with two adjacent pyramidal faces, $(10\bar{1}1)$ and $(01\bar{1}1)$, and Photo. 37 shows the side view from the direction parallel to $[\bar{1}100]$. Fig. 3 (5) is a hexagonal column with two parallel pyramidal faces, $(1\bar{1}01)$ and $(\bar{1}101)$ and Photo. 38 shows the side view of such a crystal from the direction of a_3-axis.

A special case of Fig. 3 (4) is given in Fig. 3 (6), where the area of $(10\bar{1}1)$ is smaller than that of $(01\bar{1}1)$; Photo. 39 illustrates the side view from the direction parallel to $[10\bar{1}0]$. Fig. 3 (7) is also a special case of Fig. 3 (4), the area of $(10\bar{1}1)$ being larger than that of $(01\bar{1}1)$; Photos. 40 and 41 show the side views from the direction parallel to $[10\bar{1}0]$. Figs. 3 (8-*a*) and (8-*b*) represent special cases of Fig. 3 (2). In the former case, the area of the pyramidal face $(10\bar{1}1)$ is very large, while the two prism faces $(\bar{1}100)$ and $(0\bar{1}10)$ are nearly absent. Photo. 42 shows such a crystal. In the latter case, in contrast to the former case, the area of the pyramidal face $(\bar{1}011)$ is very large; see Photo. 43.

From the foregoing illustrations of the combination of two pyramidal faces, the cases of more than two pyramidal faces can easily be inferred, as will be explained

in the following.

The special case of eight pyramidal faces is shown in Fig. 3 (9). The crystal of this type consists of two base faces, two prism faces, and eight pyramidal faces. As can be seen from the figure, the side view (Fig. 3 (9–*a*)) presents an almost complete similarity to end view (Fig. 3 (9–*b*)). Calculation by the use of BARNES' lattice model of ice[15][16], yields slightly different values for the corresponding angles as shown in the figures. But the difference is so small that it is impossible from the measurement of angles on the photographs to determine whether a side view or an end view comes into question. In view of the fact, however, that in the basal face there sometimes appear small air bubbles lying along *a*-axes, as shown in Photo. 33, it might be assumed (rather speculative though it is) that Photo. 44 represents an end view of this type of crystal.

Figs. 3 (10), (11) and (12) show a perfect shape of ice crystal, which consists of two base, six prism and twelve pyramidal faces. Photo. 45 corresponds to Fig. 3 (10) and Photos. 46 and 47 to Fig. 3 (11), which are very similar to the pointed bipyramidal crystal mentioned by HUMPHREYS[2] in his observation of halos. The crystal shape of Fig. 3 (12) can be seen in Photo. 48. A projection chart of a perfect form of ice crystal is given in Fig. 5, where the values of the angles are calculated from BARNES' lattice model of ice.

The variations in shape shown in Fig. 3 are similar to those of etch pits, which are reproduced in Fig. 4 from the previous work[7]. By way of illustration, a perfect type of etch pit is shown in Photo. 49. The etch pit may be considered as a negative

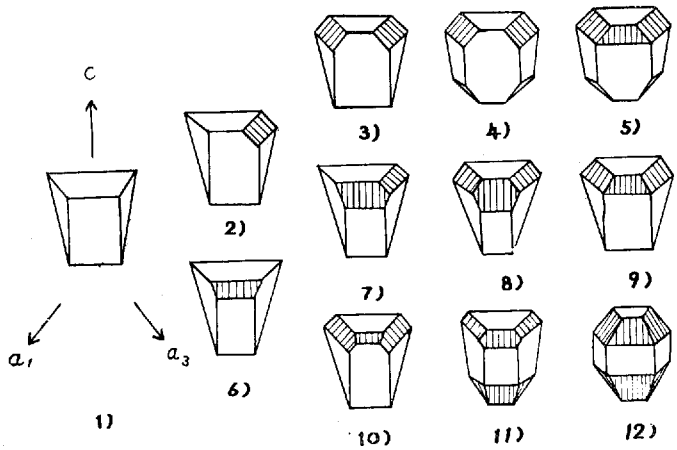

Fig. 4.

ice crystal, as is the case with the Tyndall figure, which is related to the ice crystal in water, according to NAKAYA[17].

There are some different models of the lattice structure of ice. To see which model corresponds with facts, the angles between edges (θ_1 and θ_3) and the facial

angle (θ_2), as shown schematically in Fig. 6, were measured for suitable samples: Photos. 37 and 39 corresponding to Fig. 6 (a), Photo. 35 corresponding to Fig. 6 (b), and Photos. 40 and 41 corresponding to Fig. 6 (c). It has been reasonably assumed that the crystals in these photographs have the principal axes parallel to the surface of the glass plate, so that Photos. 37, 39, 40 and 41 are the side views from the direction perpendicular to a-axis, and Photo. 35 the side view from the direction parallel to a-axis. The measured values of the angles are given in Table I, in which the values calculated from the BARNES' lattice model are also shown. Taking into account the degree of accuracy of the measurement, it may be asserted that the observed values agree with the calculated ones. Thus the conclusion follows that the pyramidal faces grow in accordance with BARNES' lattice model. The same result has been obtained by BADER[18] from the study on prismatic depth hoar

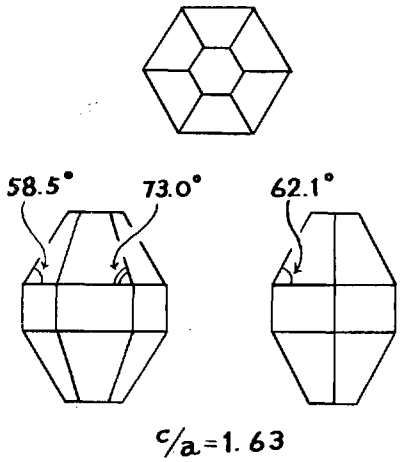

Fig. 5.

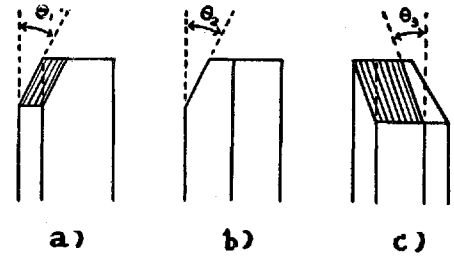

Fig. 6.

TABLE I. Measurements of the angles

Angles shown in Fig. 6	Shape of ice crystal	Angles measured (degrees)	Mean value of angles (degrees)	Angles calculated from Barnes' lattice
Fig. 6 (a)	Photo. 37	32.5	$\bar{\theta}_1 = 31.3$	31.5
		33.0		
	Photo. 39	30.0		
		29.5		
Fig. 6 (b)	Photo. 35	29.0	$\bar{\theta}_2 = 29.0$	27.9
Fig. 6 (c)	Photo. 40	21.5	$\bar{\theta}_3 = 18.0$	17.0
		18.5		
	Photo. 41	15.5		
		16.5		

crystals, by WEICKMANN[4] from the studies on ice crystals constituting the cirrostratus clouds, and also by HIGUCHI[8] from his work concerning the etch pits. It may be noticed that HUMPHREYS[2] obtained the value 24°51′ for θ_2 from his observation of halos.

V. Unusual types of ice crystals

There are to be observed in Photos. 14~31 several unusual forms of ice crystals, besides those described in the preceding section. Though not all of them could be analyzed in detail, some interesting problems will be discussed in the following.

a) Hexagonal twin prism

As seen in Photo. 41, a line perpendicular to *c*-axis is found on a certain prism face, showing that it is a hexagonal twin prism. Among the natural ice crystals in the atmosphere, the existence of twin prisms was confirmed and investigated in detail by ITOO[12]. It might be natural to assume that such twin crystals were formed in the air owing to the growth from the composition plane in two opposite directions. There is no knowing for the moment whether or not that explanation can be applied to the present case. We shall not be able to say anything definite about the origin of twins, until the growing process will actually become observable through a microscope.

In some instances, the two single crystals constituting a twin crystal show some diversity in shape. Photos. 50~56 show such crystals. In most cases twin crystals that developed in free space show perfect symmetry, from which it is suggested that the asymmetry observed in our case may be due to the difference in conditions under which the crystals grew on the glass plate. In some particular instances, as shown in Photos. 55 and 56, one component of a twin crystal appears to be composed of two crystals.

b) Irregular shapes of column crystals

There are also many crystals, having the shape of an oblique cross section of a hexagonal column. Similar cases have been reported by ADAMS[19], YOSIDA[20], NAKAYA and HANAZIMA[21], WEICKMANN[22], KOBAYASHI[23] and ITOO[6]. The analysis of the data, by the projection method, inclusive of those obtained by ITOO and WEICKMANN, will be described elsewhere[24].

VI. Summary

During experiments on snow-crystal habit by means of a diffusion cloud chamber, a number of interesting types of hoar crystals were found on a slide glass treated with Dri-film and set against the inside wall of the chamber. The conditions under which these crystals were formed are fully described and their photomicrographs are shown in Photos. 1 and 9~31.

A brief account of an analysis of crystal shapes is given with respect to several

hoar crystals having pyramidal faces. As shown in Fig. 3 and Photos. 32~48 there are several variations of hexagonal column with pyramidal faces. Comparison of Fig. 3 with Fig. 4 indicates that the shapes of these crystals are closely related to those of the etch pits formed on ice-crystal surfaces, which fact is of special interest from the crystallographical viewpoint, since it bears a similarity to the relation existing between ice crystals in water and Tyndall figures.

In some cases, the edge and facial angles could be measured on the photographs and compared with the values calculated from the BARNES' lattice model of ice, as shown in Table I. Agreement between observed angles and the calculated ones shows that the pyramidal face corresponds with BARNES' lattice. Some illustrations of hexagonal twin crystals are given in Photos. 50~56.

As for the mechanism of the appearance of pyramidal faces, no theoretical interpretation can be given at the present stage.

The workers wish to express their hearty thanks to Mr. J. MUGURUMA for the photograph of etch pits he kindly offered to them.

References

1 SCORESBY, W. 1820 An account of the Arctic regions, with a history and description of the northern whale-fishery. Edinburgh.

2 HUMPHREYS, W. J. 1940 Physics of the air. McGraw-Hill Book Co., 534~536.

3 NAKAYA, U. 1954 Snow crystals natural and artificial. Harvard University Press.

4 WEICKMANN, H. 1947 Die Eisphase in der Atmosphäre (The ice phase in the atmosphere). Berichte des Deutschen Wetterdienstes in der US-Zone, Nr. 6. Royal Aircraft Establishment, Library Translation No. 273, (1948).

5 SHAW, D. and MASON, B. J. 1955 The growth of ice crystals from the vapour. Phil. Mag., **46**, 249~262.

6 ITOO, K. 1956 To be published.

7 KOBAYASHI, T. 1957 Experimental researches on the snow-crystal habit and growth by means of a diffusion cloud chamber. To be published in 75 th Anniversary Volume, Journ. Meteor. Soc. Japan.

8 HIGUCHI, K. 1955 The etching of ice crystals. In press.

9 KOBAYASHI, T. 1956 Experimental researches on the snow-crystal habit and growth by means of a diffusion cloud chamber (Preliminary report). Low Temp. Sci., Ser. A, **15**, 1~11. (in Japanese).

10 NAKAYA, U., SUGAYA, J. and SHODA, M. 1957 Report of the Mauna Loa expedition in the winter of 1956~57. Journ. Fac. Sci. Hokkaido Univ., Ser. II, **5**, 1~35.

11 SCHAEFER, V. J. 1951 Snow and its relationship to experimental meteorology. Compendium Meteor. Boston, Amer. Meteor, Soc., 225.

12 ITOO, K. 1953 Forms of ice crystals in the air. Papers in Meteor. and Geophys., **3**, 207~216.

13 NAKAYA, U. 1954 Reference *3*, 50.

14 NAKAYA, U. 1954 Reference *3*, 219~220.

15 BARNES, W. H. 1929 The crystal structure of ice between 0°C and −183°C. Proc. Roy. Soc., A. **125**, 670~693.

16 OWSTON, P. G. and LONSDALE, K. 1948 The crystal structure of ice. Journ. Glaci., **1**, 118~123.

17 NAKAYA, U. 1956 Properties of single crystals of ice, revealed by internal melting. S. I. P. R. E. Research Paper, **13**.

18 BADER, H. et al. 1939 Der Schnee und seine Metamorphose (Snow and its metamorphism). Beiträge zur Geologie der Schweiz, Geotechnische Serie, Hydrologie, Lieferung 3. S. I. P. R. E., Translation 14, (1954).

19 ADAMS, J. M. 1930 The polar properties of single crystal of ice. Proc. Roy. Soc., A, **128**, 588~590.

20 YOSIDA, Z. 1939 Window hoar crystals on clean glass surfaces. Journ. Fac. Sci. Hokkaido Imp. Univ., Ser. II, **3**, 43~55.

21 NAKAYA, U. and HANAZIMA, M. 1950 Frost flower. Kotori-shorin, Kyoto, 58~59. (in Japanese).

22 WEICKMANN, H. 1947 Reference *4*, Figs. 45~48.

23 KOBAYASHI, T. 1954 Studies on small ice crystals II. On the ice crystals formed on hydrophobic substances; A general survey. Contrib. Inst. Low Temp. Sci., No. 6, 7~18.

24 HIGUCHI, K. 1957 Determination of faces of ice crystals by the method of projection. To be published in Journ. Meteor. Soc. Japan.

PLATE I.

Photo. 1. (× 90 :)

Hoar crystals formed on the slide glass treated with Dri-film.

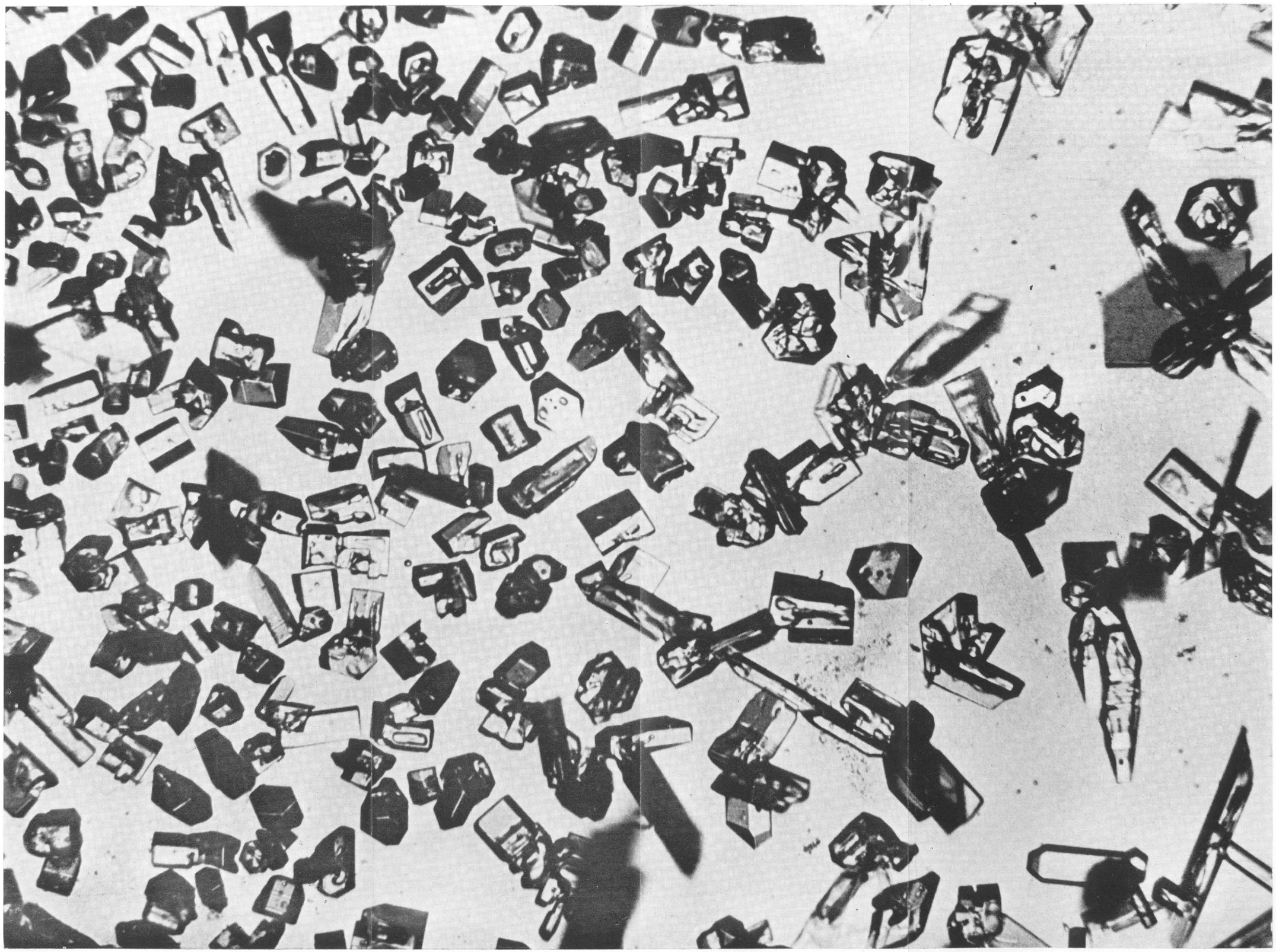

PLATE II.

Snow crystals produced under the influence of silicone oil.

Photo. 2. Sheath-type crystals produced under the influence of vapour trace of methyl silicone oil (KF 96, 5 c.s.).
(× 7.1 ; T_a* = −13.5°C.)

Photo. 3. Ditto, (TS 951, 0.65 c.s.).
(× 18 ; T_a = −16.9°C.)

Photo. 4. Sheath and needle crystals produced under the influence of Dri-film vapour.
(× 16 ; T_a = −25.2°C.)

Photo. 5. A peculiar type of crystals developed from a silk thread wetted with silicone oil (DC 200, 100 c.s.),
(× 5.6 ; T_a = −18°C.)

Photo. 6. A curious shape of a *pseudo-dendritic* crystal produced under the influence of the vapour of Toshiba methyl-phenyl silicone oil, 6 c.s.
(× 6.4 ; T_a = −13°C.)

Photo. 7. Ditto.
(× 18 ; T_a = −12.6°C.)

---

* The temperature of the air where the crystal is formed.

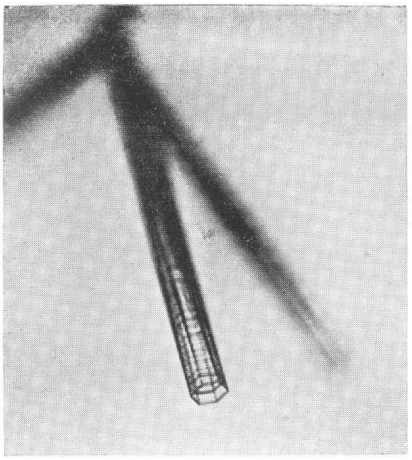

2

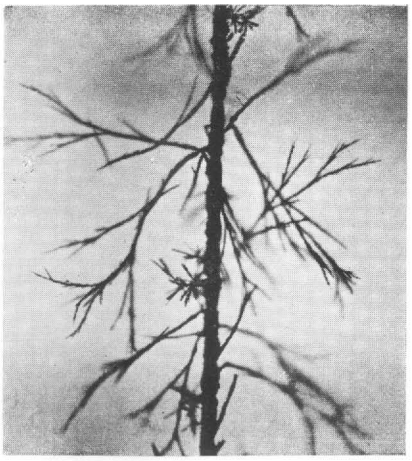

5

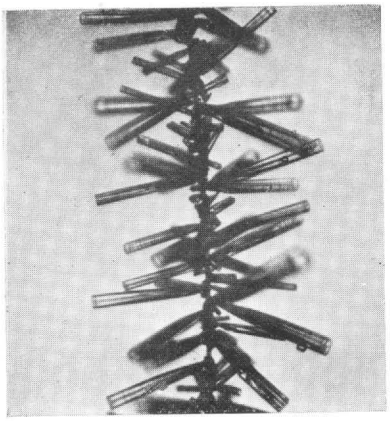

3

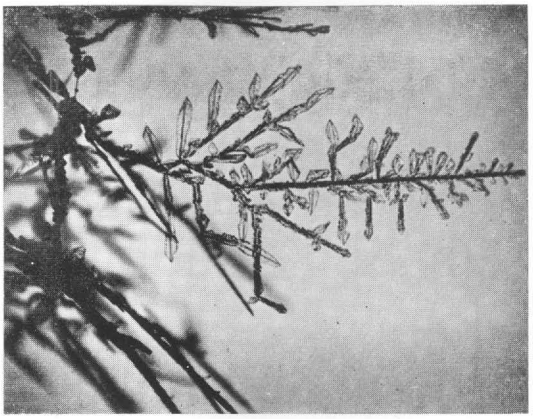

6

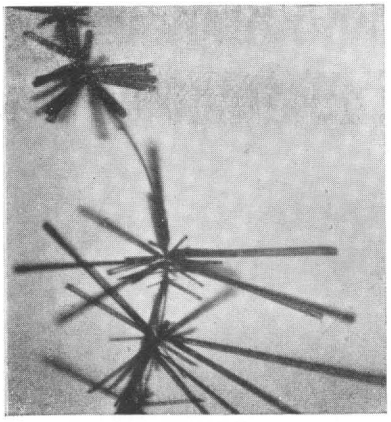

4

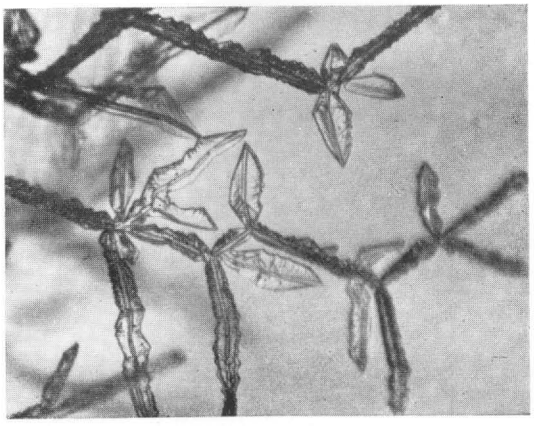

7

PLATE III.

Photo. 8. (× 6.4 :)

Needle crystals formed in region (*A*) on the slide.

Photos. 9～13. (× 15 :)

Clumps of columnar crystals in region (*C*).

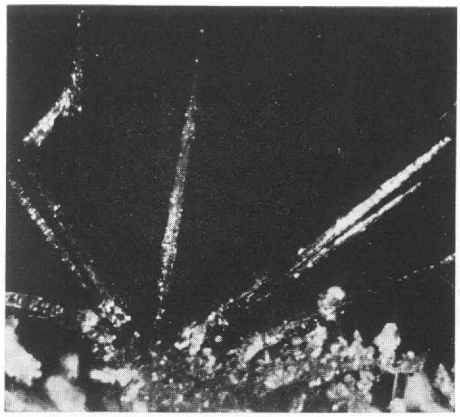

8

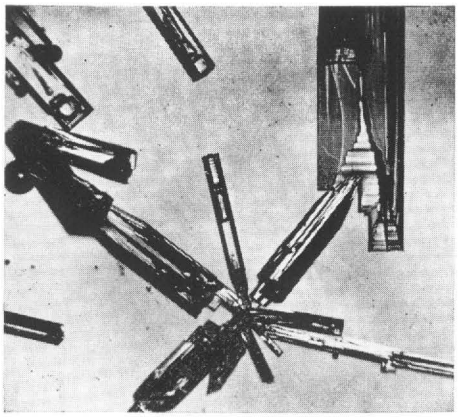

9

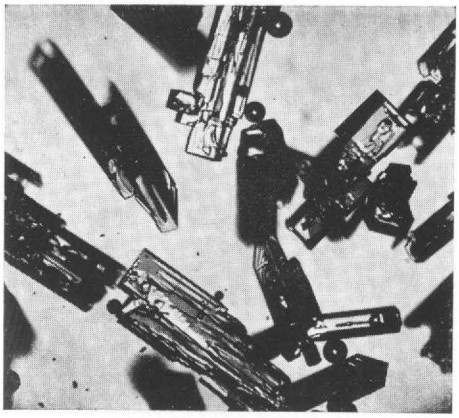

10

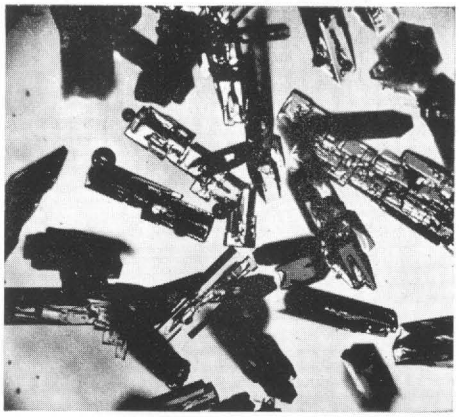

11

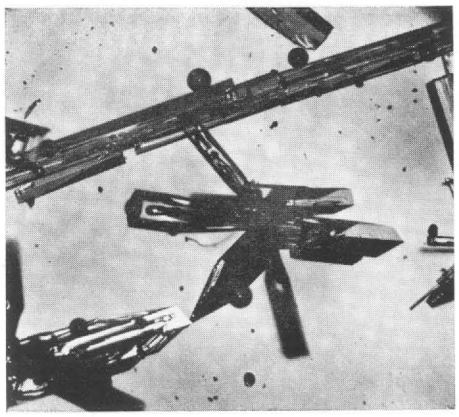

12

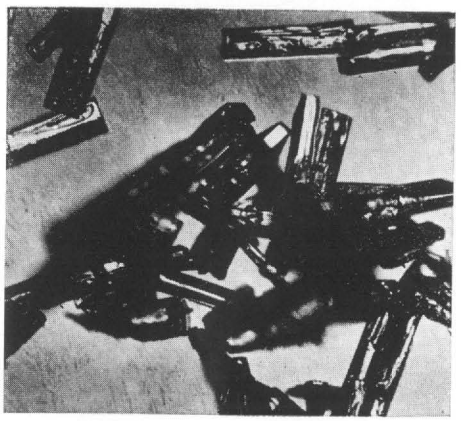

13

PLATE IV.

Photos. 14 and 15. (× 29 :)

Low-magnification-microscope views of region (*B*) on the slide.

Various types of crystals bounded by pyramidal faces can be seen.

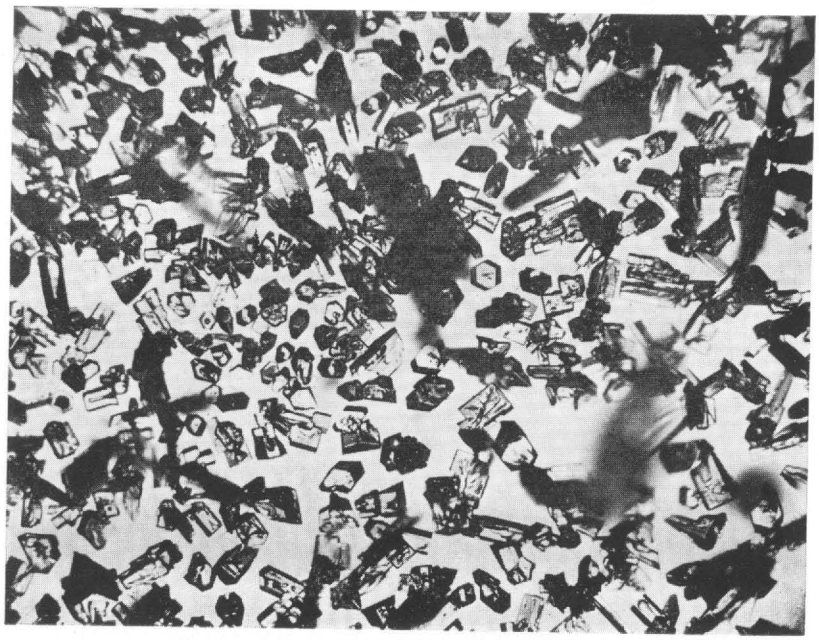

14

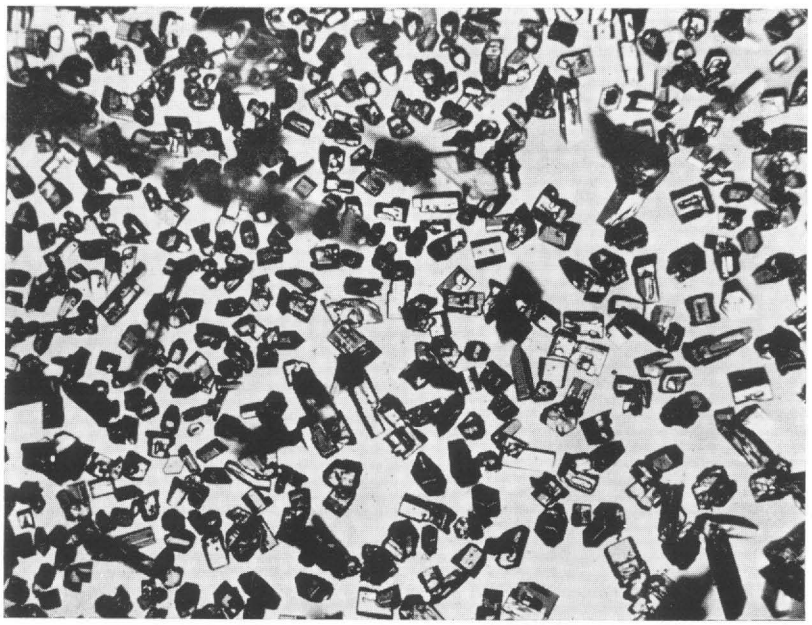

15

PLATE V.

Photos. 16 and 17. (× 29 :)

Low-magnification-microscope views of region (*B*) on the slide.

Various types of crystals bounded by pyramidal faces can be seen.

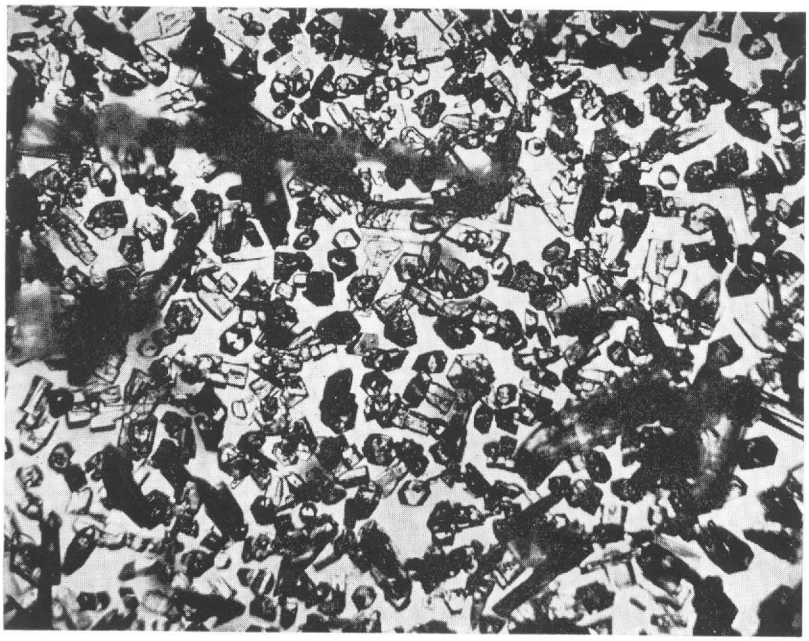

16

17

PLATE VI.

Photos. 18 and 19. (× 29:)

Low magnification views of region (*C*) on the same slide as shown in Photos. 14~17.

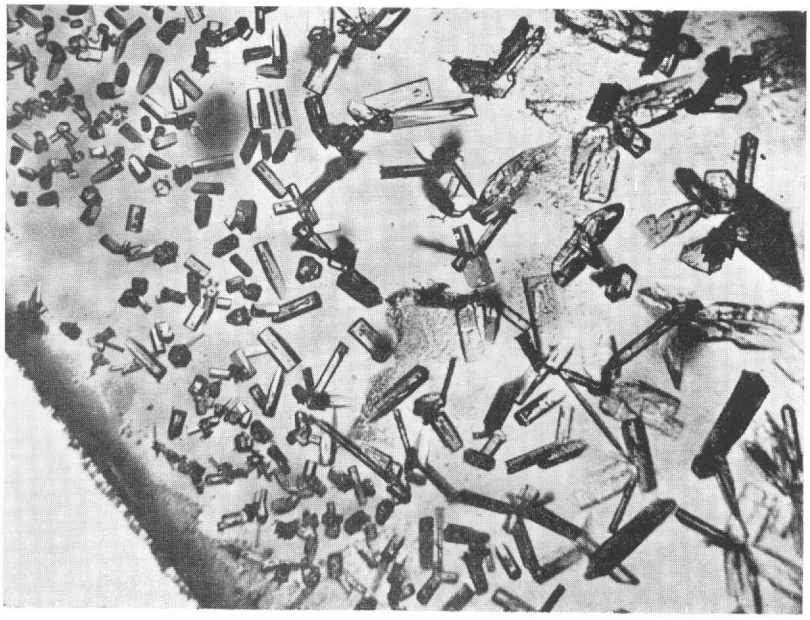

18

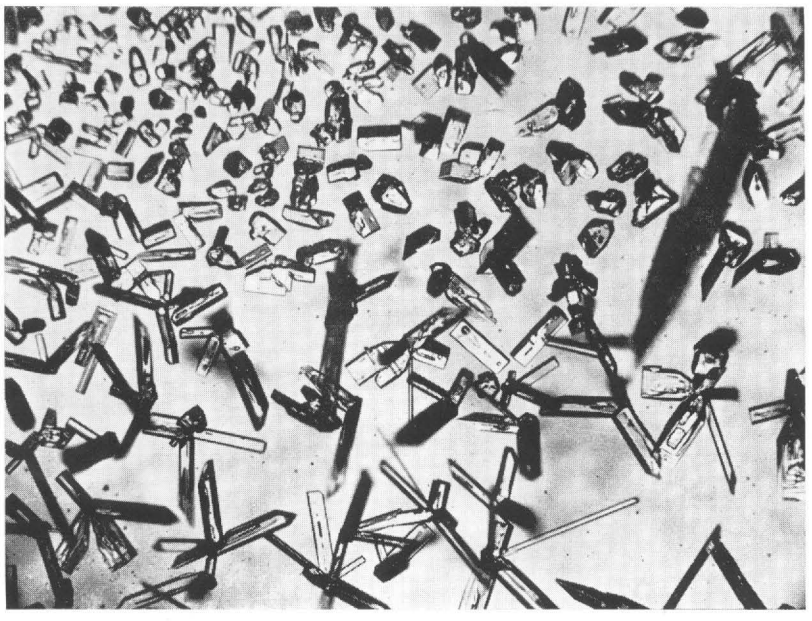

19

PLATE VII.

Photos. 20～23. (× 55 :)

Higher magnification views of crystals observed in the region (*B*) on the same slide as shown in Photos. 14～17 or the like.

20

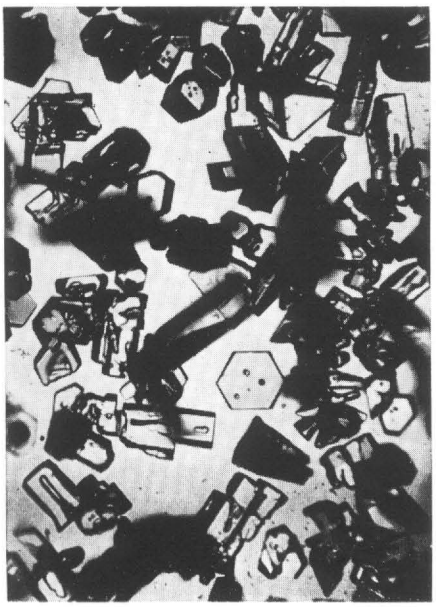

21

22

23

PLATE VIII.

Photos. 24~27. (× 55 :)

Higher magnification views of crystals observed in the region (*B*) on the same slide as shown in Photos. 14~17 or the like.

24

25

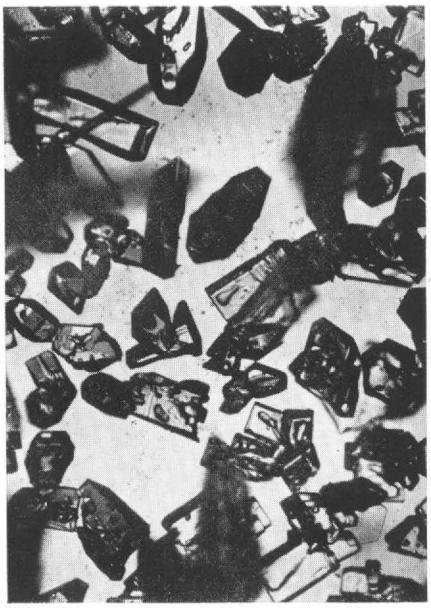

26

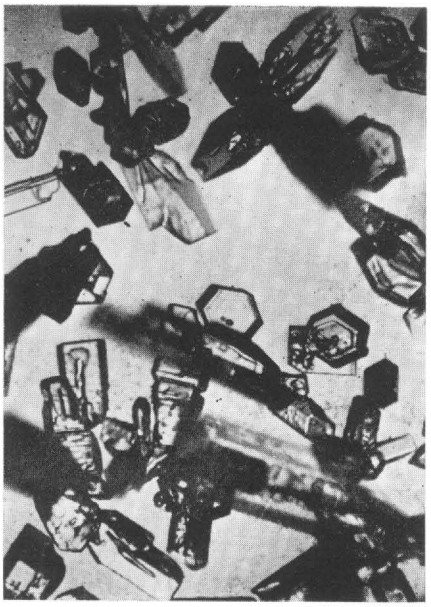

27

PLATE IX.

Photos. 28 and 29. ($\times$ 55 :)

Higher magnification views of crystals in region (*B*).

Photos. 30 and 31. ($\times$ 55 :)

Higher magnification views of crystals in region (*C*). Side views of columnar or needle-like crystals.

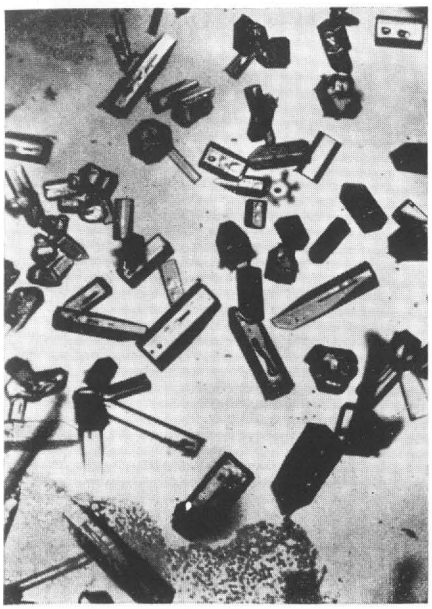

28

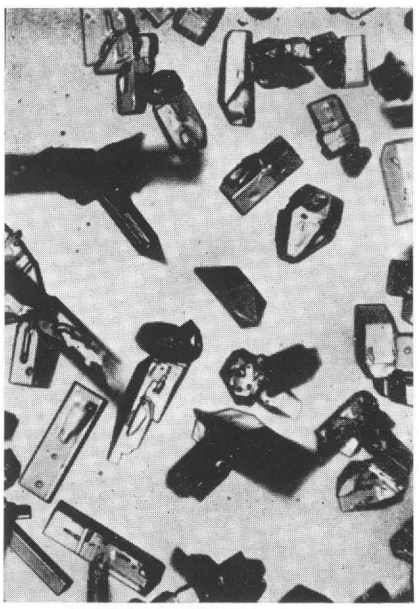

29

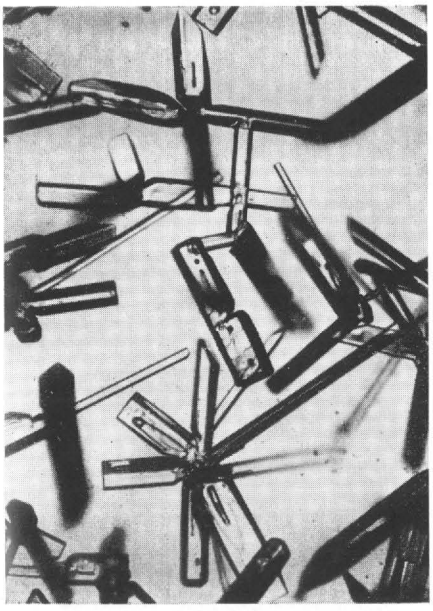

30

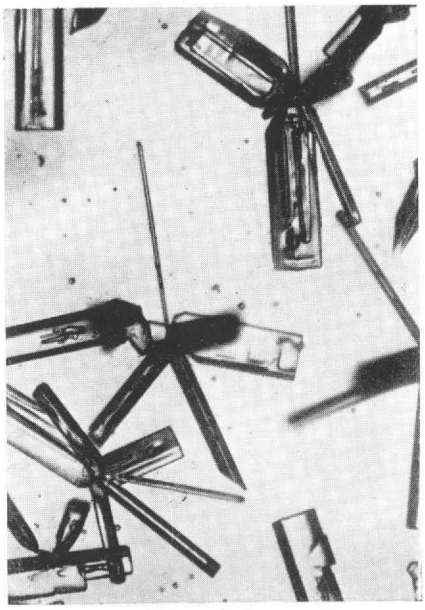

31

PLATE X.

Photo. 32. (× 155 :)

Column crystal, corresponding to Fig. 3 (1).

Photo. 33. (× 132 :)

Column crystal, corresponding to Fig. 3 (1). (end view.)

Photo. 34. (× 175 :)

Column crystal with one pyramidal face, corresponding to Fig. 3 (2).

Photo. 35. (× 155 :)

Column crystal with one pyramidal face (side view from the direction parallel to *a*-axis), corresponding to Fig. 3 (2).

Photo. 36. (× 155 :)

Column crystal with two pyramidal faces, $(1\bar{1}01)$ and $(01\bar{1}1)$, corresponding to Fig. 3 (3).

Photo. 37. (× 167 :)

Column crystal with two pyramidal faces, $(10\bar{1}1)$ and $(01\bar{1}1)$ (side view from the direction parallel to $[\bar{1}100]$), corresponding to Fig. 3 (4).

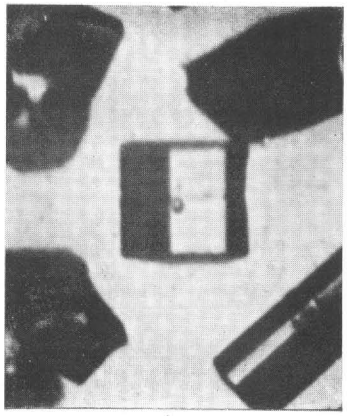

32

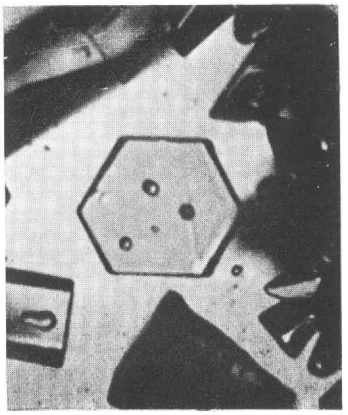

33

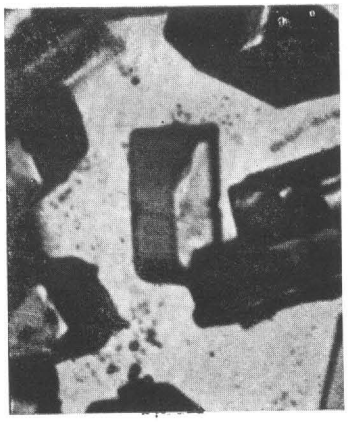

34

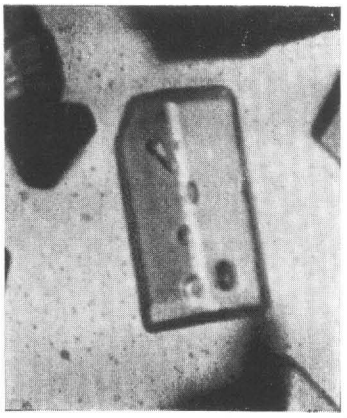

35

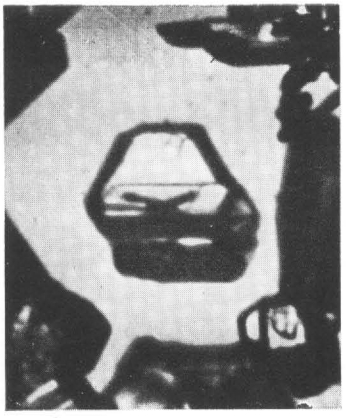

36

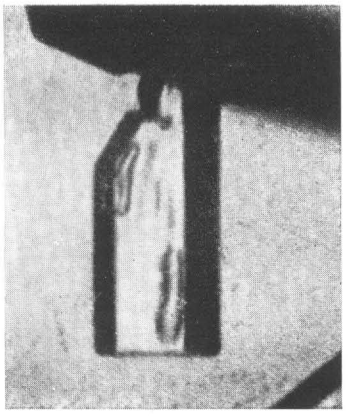

37

PLATE XI.

Photo. 38. (× 155 :)

Column crystal with two parallel pyramidal faces, $(1\bar{1}01)$ and $(\bar{1}101)$ (side view from the direction parallel to a_3-axis), corresponding to Fig. 3 (5).

Photo. 39. (× 155 :)

Column crystal with large $(01\bar{1}1)$ face (side view from the direction parallel to $[10\bar{1}0]$), corresponding to Fig. 3 (6).

Photo. 40. (× 155 :)

Column crystal with large $(10\bar{1}1)$ face (side view from the direction parallel to $[\bar{1}010]$), corresponding to Fig. 3 (7).

Photo. 41. (× 155 :)

Column crystal similar to Photo. 40.

Photo. 42. (× 198 :)

Column crystal with large $(10\bar{1}1)$ face, corresponding to Fig. 3 (8–a).

Photo. 43. (× 155 :)

Column crystal with large $(\bar{1}011)$ face, corresponding to Fig. 3 (8–b).

Photo. 44. (× 132 :)

Column crystal with eight pyramidal faces (end view), corresponding to Fig. 3 (9).

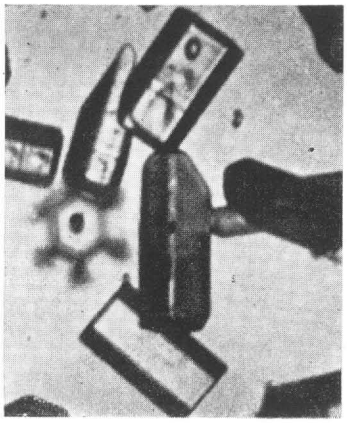

38

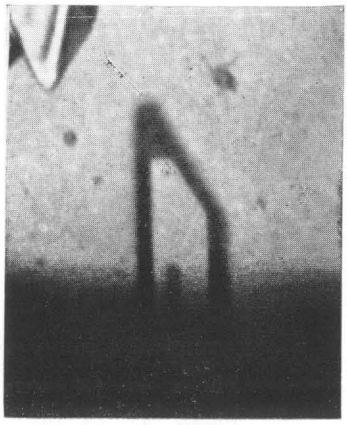

39

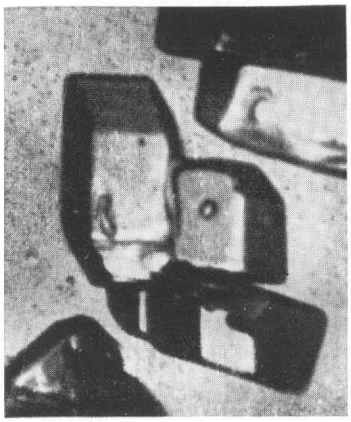

40

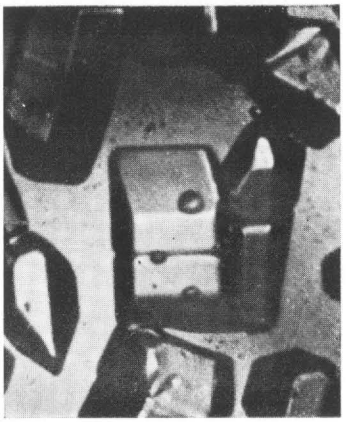

41

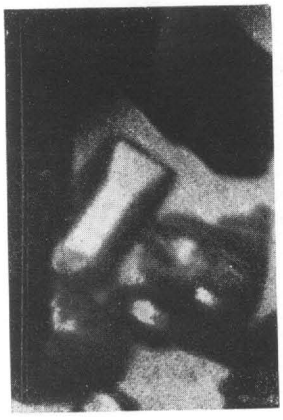

42

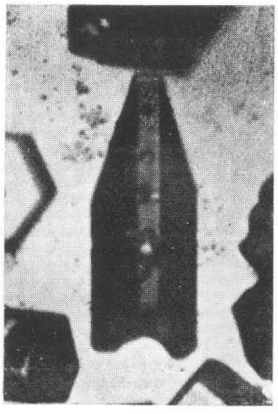

43

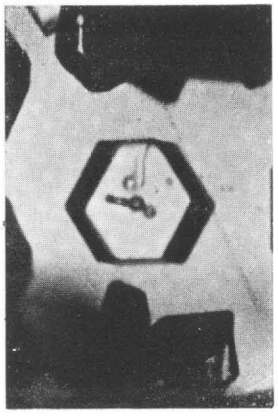

44

PLATE XII.

Photo. 45. (× 195 :)

A part of pyramidal column crystal, corresponding to Fig. 3 (10).

Photos. 46 and 47.

Bipyramidal column crystals, corresponding to Fig. 3 (11).

Photo. 46 (× 155 :)

Photo. 47 (× 198 :)

Photo. 48. (× 155 :)

Perfect shape of bipyramidal column crystals, corresponding to Fig. 3 (12).

Photo. 49. (× 50 :)

Perfect shape of etch pit produced on the surface of bulk ice, corresponding to Fig. 4 (12). (after Mr. MUGURUMA)

Photo. 50. (× 155 :)

Hexagonal twin crystal.

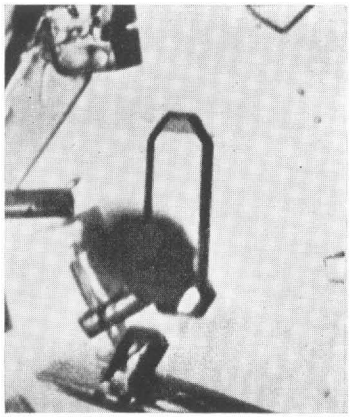

45

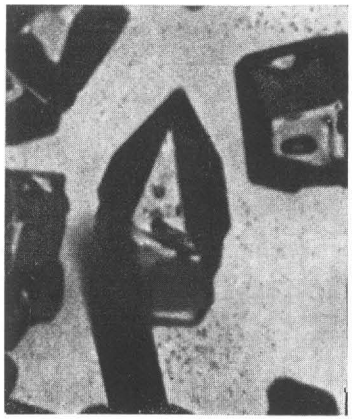

46

47

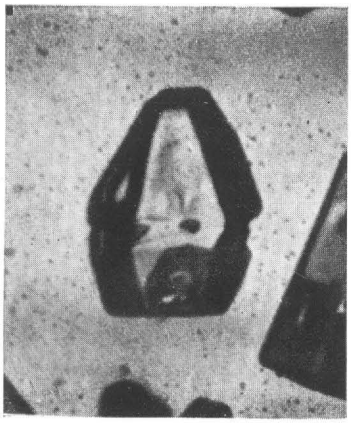

48

49

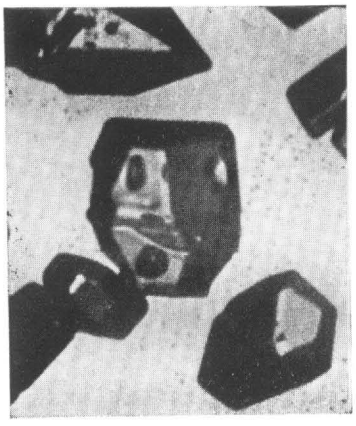

50

PLATE XIII.

Photos. 51～54.

Several shapes of hexagonal twin crystals.

Photo. 51 (× 155 :)

Photo. 52 (× 198 :)

Photo. 53 (× 116 :)

Photo. 54 (× 132 :)

Photos. 55 and 56. (× 155 :)

Hexagonal twin crystals, one component of which appears to be constituted of two crystals.

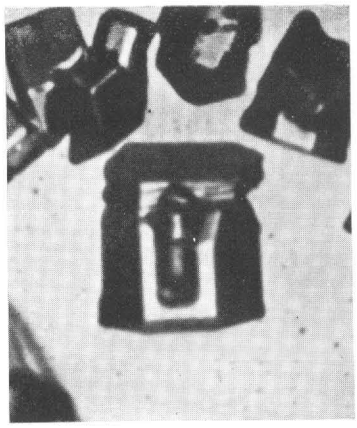

51

52

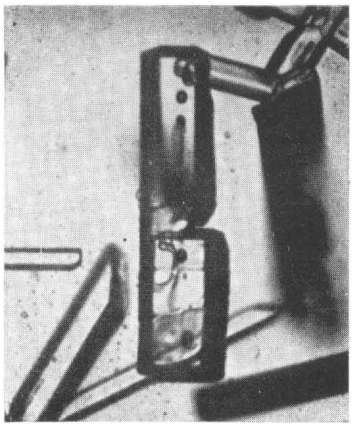

53

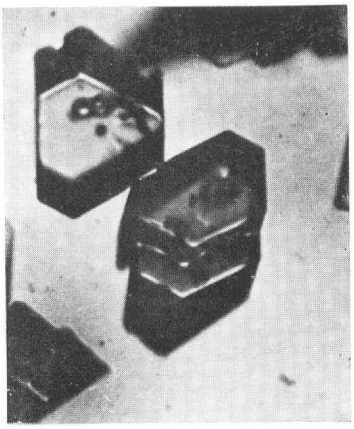

54

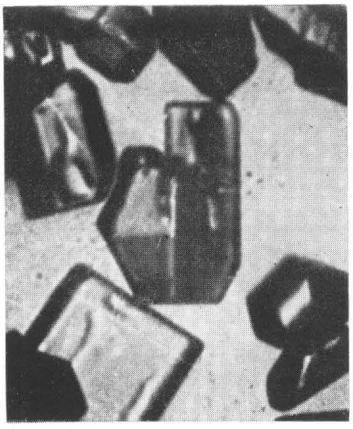

55

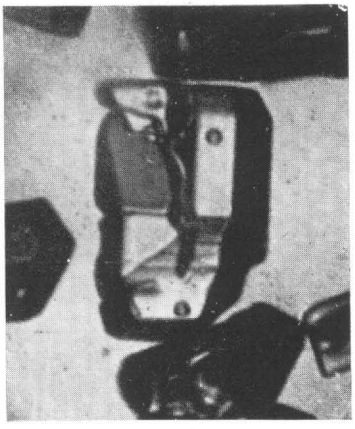

56